Evaluation and Spectral Analysis of a Locally Refined EGM96 "EGM96EGR" Harmonic Model

Dr. Maher Mohamed Amin[1] ***Dr. Saadia Mahmoud El-Fatairy***[1]
Eng. Raaed Mohamed Hassouna[2]
[1] *Lecturer of Surveying, Surveying Department, Shoubra Faculty of Engineering, Zagazig University*
[2] *Assistant Lecturer, Civil Engineering Department, Faculty of Engineering in Shebin El-Kom, Menoufia University*

Abstract:

The EGM96 harmonic model was previously refined to match Egypt better, based on the local gravity data in Egypt, by collocation. The refined model was given the name EGM96EGR. In the current study, the EGM96EGR model was compared with the EGM96 model, regarding the relevant harmonic coefficients as well as the associated error estimates. In addition, the two models were compared in terms of the relevant computed low degree geoidal heights, gravity anomalies and deflection components in the Egyptian territory. The comparison showed very significant differences between the two models. Again they were compared in two far test areas, one with and the other without data contribution to the EGM96 model. The discrepancy between the two models in both areas was found to be insignificant. A global spectral analysis was performed, involving the power spectra (degree variances) and error spectra, based on the coefficients and standard errors pertaining to both the refined and original model. Small differences were detected between the two models regarding the power spectra. However, the error degree variances (error spectra) of the refined model were greater than those of the original one.

1 Introduction

In local gravity field modeling, the long wavelength information is a necessity. This can be obtained via a global geopotential model as a reference field. In this manner, not only the truncation error is reduced, but also the computational effort, which would theoretically involve the whole globe, is much limited. However, the long wavelength information could be reliably extracted from such harmonic model, only if it had local terrestrial gravity data contribution from the region under investigation. Unfortunately, the Egyptian terrestrial gravity data till now has not been incorporated in any of the several solutions for such global harmonic models (Amin, 2002). Hence, in a previous study made by the authors (Amin etal., 2002), the EGM96, as a high quality and high-resolution harmonic model (Lemoine et al., 1996), was refined to fit Egypt better. The refinement based on using the local residual gravity data to predict low frequency corrections for the relevant spherical harmonic coefficients of the EGM96 model. Using the refined model as a reference field, an improvement of about 40% was achieved over the original model, regarding the local anomaly field smoothing. The general approach of the prediction of harmonic coefficients and their error estimates by collocation was thoroughly investigated and tested in (Tscherning, 2001).

2002, *Port-Said Engineering Research Journal PSERJ, Vol. 6 No.(2), Published by Faculty of Engineering, Suez Canal University, Port-Said, Egypt*

In the current investigation, the two models (the original and the refined) were compared, concerning the differences among the relevant harmonic coefficients as well as their associated error estimates. A further comparison was held, regarding their low frequency information at the nodes of 0.5˚X0.5˚ grids in Egypt and in two test zones far from Egypt. The first far geographical zone has local data contribution to the EGM96 model (Kearsley et al., 1998), whereas the second one does not. The comparison involved the low degree geoidal heights, gravity anomalies and deflection components. Within the Egyptian region, for which the model was refined, very significant differences resulted between the refined and the original model, concerning all the four anomalous quantities. Conversely, both the two far zones exhibited very small discrepancies between the gravimetric quantities computed from the two models.

A spectral analysis was also performed for both the EGM96 and the EGM96EGR models involving degree variances (power spectra) and error degree variances (error spectra), based on the relevant harmonic coefficients and their associated standard errors, respectively. Namely, the coefficient, geoid and gravity anomaly power and error spectra were evaluated for the spectral range from degree 2 to 360. Small randomly oscillating (and damping) differences were observed among the power spectra, relevant to the refined and original model. However, the error spectra associated with the EGM96EGR model were considerably greater than that of the EGM96.

2 Background

It is well known that when using a global harmonic model of a resolution up to degree and order 360, the relevant low degree gravimetric quantities, T, N, Δg, ξ and η, can be expressed by the following formulas

$$T(\psi,\lambda,r) = (GM/r) \sum_{n=2}^{360} (a/r)^n \sum_{m=0}^{n} (\bar{C}^{*}_{nm} \cos m\lambda + \bar{S}_{nm} \sin m\lambda) \bar{P}_{nm}(\sin\psi) \quad (1)$$

$$N(\psi,\lambda,r) = (GM/r\gamma) \sum_{n=2}^{360} (a/r)^n \sum_{m=0}^{n} (\bar{C}^{*}_{nm} \cos m\lambda + \bar{S}_{nm} \sin m\lambda) \bar{P}_{nm}(\sin\psi) \quad (2)$$

$$\Delta g(\psi,\lambda,r) = (GM/r^2) \sum_{n=2}^{360} (n-1) (a/r)^n \sum_{m=0}^{n} (\bar{C}^{*}_{nm} \cos m\lambda + \bar{S}_{nm} \sin m\lambda) \bar{P}_{nm}(\sin\psi) \quad (3)$$

$$\xi(\psi,\lambda,r) = - (GM/r^2\gamma) \sum_{n=2}^{360} (a/r)^n \sum_{m=0}^{n} (\bar{C}^{*}_{nm} \cos m\lambda + \bar{S}_{nm} \sin m\lambda) d\bar{P}_{nm}(\sin\psi)/d\psi \quad (4)$$

$$\eta(\psi,\lambda,r) = - (GM/r^2\gamma\cos\psi) \sum_{n=2}^{360} (a/r)^n \sum_{m=0}^{n} m(\bar{C}^{*}_{nm} (-\sin m\lambda) + \bar{S}_{nm} \cos m\lambda) \bar{P}_{nm}(\sin\psi) \quad (5)$$

where

T, N, Δg, ξ and η are the relevant computed anomalous potential, geoidal height, gravity anomaly, deflection component in the meridian direction and deflection component in the prime vertical direction, respectively,

ψ the geocentric latitude,

λ the geodetic longitude,

r the geocentric radius to the geoid,

$\gamma(\psi,r)$ the normal gravity implied by the reference ellipsoid,

GM the Earth mass gravitational constant,

a the equatorial radius,

$\bar{C}^{*}_{nm}$ the fully normalized spherical harmonic C-coefficients of degree n and order m, reduced for the even zonal harmonics of the reference ellipsoid,

$\bar{S}_{nm}$ the fully normalized spherical harmonic S-coefficients of degree n and order m,

$\bar{P}_{nm}(\sin\theta)$ the fully normalized associated Legendre function of degree n and order m.

The magnitudes of spherical harmonic coefficients are generally randomly damping as the degree increases. The square of any of the above expansions, at a specific degree, yields a relevant positive real number, which is referred to as the degree variance. This is evident from the orthogonality among the coefficients on one hand and among the surface harmonic functions on the other hand (Heiskanen and Moritz, 1967). Most common, however, are the geoid, anomaly and coefficient degree variances. The (positive) degree variance expresses how much signal power (content) is implied by all the coefficients belonging to a specific degree, in a global sense. It is usually referred to as the power spectrum. Hence, the variation of power spectra with the degree describes in a practical way the rate of decay of the anomalous signal as the degree increases. The geoid, gravity anomaly and coefficient spectra (degree variances) are, respectively, given (in spherical approximation) as

$$(\sigma^2_n)_N = (R)^2 \sum_{m=0}^{n} (\bar{C}^{*2}_{nm} + \bar{S}^2_{nm}) \qquad (6)$$

$$(\sigma^2_n)_{\Delta g} = (G')^2 .(n-1)^2. \sum_{m=0}^{n} (\bar{C}^{*2}_{nm} + \bar{S}^2_{nm}) \qquad (7)$$

$$(\sigma^2_n)_{C:S} = \sum_{m=0}^{n} (\bar{C}^{*2}_{nm} + \bar{S}^2_{nm}) \qquad (8)$$

where R and G' are the mean radius of the Earth and the mean gravity, respectively. If the harmonic coefficients in the above formulas are replaced with their error estimates, σ_{C^*nm} & σ_{Snm}, one obtains the so-called error degree variances (error spectra). Thus, one obtains the geoid, anomaly and coefficient error degree variances as follows

$$(\sigma_{e}^{2}{}_{n})_{N} = (R)^2 \sum_{m=0}^{n} (\sigma^2_{C^*nm} + \sigma^2_{Snm}) \tag{9}$$

$$(\sigma_{e}^{2}{}_{n})_{\Delta g} = (G')^2 .(n-1)^2. \sum_{m=0}^{n} (\sigma^2_{C^*nm} + \sigma^2_{Snm}) \tag{10}$$

$$(\sigma_{e}^{2}{}_{n})_{C:S} = \sum_{m=0}^{n} (\sigma^2_{C^*nm} + \sigma^2_{Snm}) \tag{11}$$

The (positive) error degree variance expresses how much signal power error of a given anomalous quantity exists, in a global sense, for all the coefficients of a specific degree. In general, the error degree variances and degree variances are very useful in covariance function modeling (Tscherning, 1993).

3 Harmonic coefficients and their uncertainties

Figures (1a) and (1b) show two gray scaled contour maps for the corrections applied to the EGM96 C and S-coefficients, respectively, from degree and order 2,0 to degree and order 360. The numerical levels of the corrections as well as the contour interval could be deduced from the gray scale. These graphical plots were outlined for the sake of an objective and detailed overview of the corrections received by the various spectral domains. Clearly, very significant values for the corrections could be recovered. However, the corrections for the sectorial (m=n) and near sectorial (m≈n) harmonic coefficients were negligible for most of the high degrees. These negligible corrections were more pronounced, in both magnitude and number after degree and order 150. Thus the relevant coefficients could be very well represented by the EGM96 model, or the Egyptian data could be poor in these terms, due to their geographical location. The coefficients from degree and order (2,0) to (10,10) have received very small corrections, but within the number of significant figures of the original coefficients. Finally, one can easily notice that the two maps are similar.

Figures (2a) and (2b) show two maps for the standard errors of the EGM96 model C and S-coefficients, respectively. The two maps are similar. One can easily distinguish between two spectral bands with different error characteristics. The first band is obviously from degree and order 2,0 to degree and order 70, whereas the second error band ranges between degree and order 71,0 to degree and order 360. The first region begins with very small values for the standard errors, then a hill appears in the middle of that region and the errors decrease to reach a local minimum at degree 70. A sudden

jump, which is independent on the order, occurs at degree 70. In the second stage the standard errors decreases as the degree increases, with a slight dependence on the coefficients' orders. The jump at degree 70 is an indication that the high quality start 70,70 satellite terms, although they were mixed with global mean terrestrial data in the solution steps for the EGM96 model, these terms has preserved their own error characteristics. As the coefficients' magnitudes are in general damping as the degree increases, the second trend of the standard errors ensures the high quality of the EGM96 harmonic model. Namely, the damping coefficients have acceptable decreasing error estimates.

Figures (3a) and (3b) plot two maps for the standard errors of the EGM96EGR model C and S-coefficients, respectively. As above, the two maps are similar. Also two spectral bands with different error characteristics manifest themselves. The first band is obviously from degree and order 2,0 to degree and order 70, whereas the second error band ranges between degree and order 71,0 to degree and order 360. The main features of the contour lines in both trends, however, are fully independent on the coefficients' orders. The first region begins with very small values for the standard errors, then a local maximum appears in the middle of that region and the errors decrease to reach a local minimum at degree 70. Again, a sudden jump, which is also independent on the order, occurs at degree 70. In the second stage, the standard errors decrease gently as the degree increases. These latter two maps show, in general, how efficiently the original model (scaled) error degree variances have succeeded in modeling the covariance function (Tscherning, 1993), prior to the solution for the coefficients' corrections. This is evident, because the error estimates scheme of the EGM96EGR coefficients resembles to a great extent that pertaining to the original model.

In general, although the least-squares estimation of spherical harmonic coefficients results in coefficients' values that are quite consistent with the input information, the associated coefficients error estimates are of a rather pessimistic nature. This can be related to the fact that the computation of the coefficients error estimates by least-squares collocation, using an isotropic covariance function, is based on the assumption that the coefficients pertaining to a specific degree all belongs to the same normal distribution (Tscherning, 2001). This affects more the lower degrees. This is evident because the larger the degree, the more is the number of relevant coefficients, and hence, the more realistic is the normal distribution hypothesis. Thus, the rapid decrease of the error estimates, in the second error band, as the degree increases could be, among other factors, related to this effect. This can also be considered in general as the main reason, why the resulting error estimates for the refined coefficients are larger than those of the original coefficients. Moreover, the merely dependence of the error estimates on the degree in Figures (3a) and (3b) could be regarded to that statistical ambiguity, since the coefficients belonging to a specific degree have their own statistical characteristics.

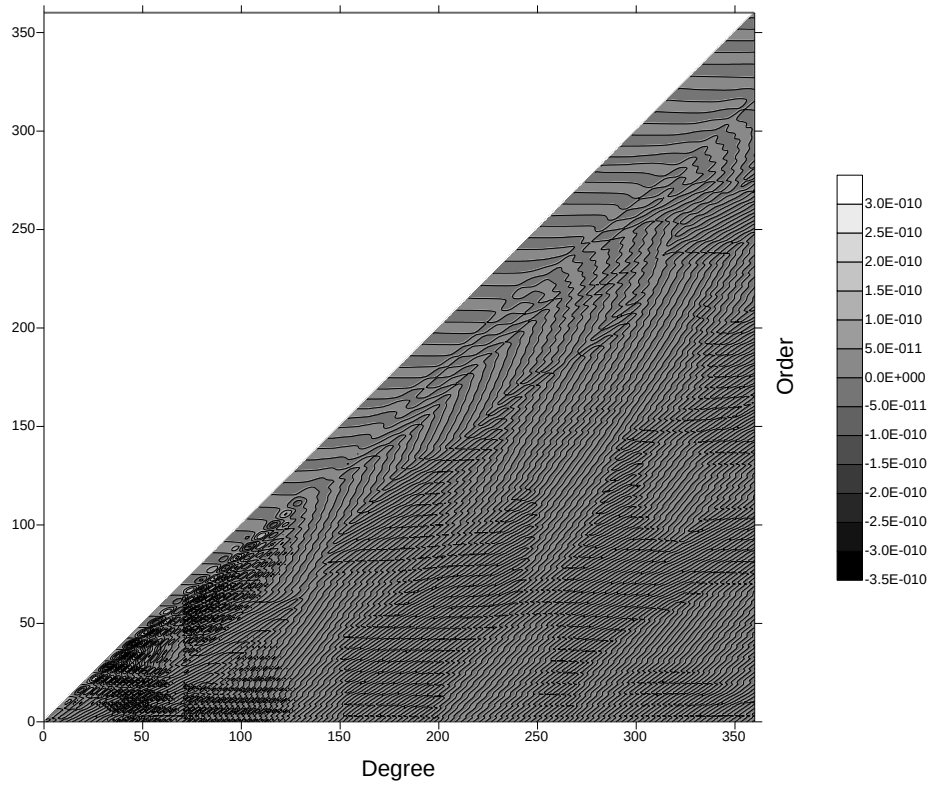

Figure (1a): Contour map for the EGM96 C-corrections

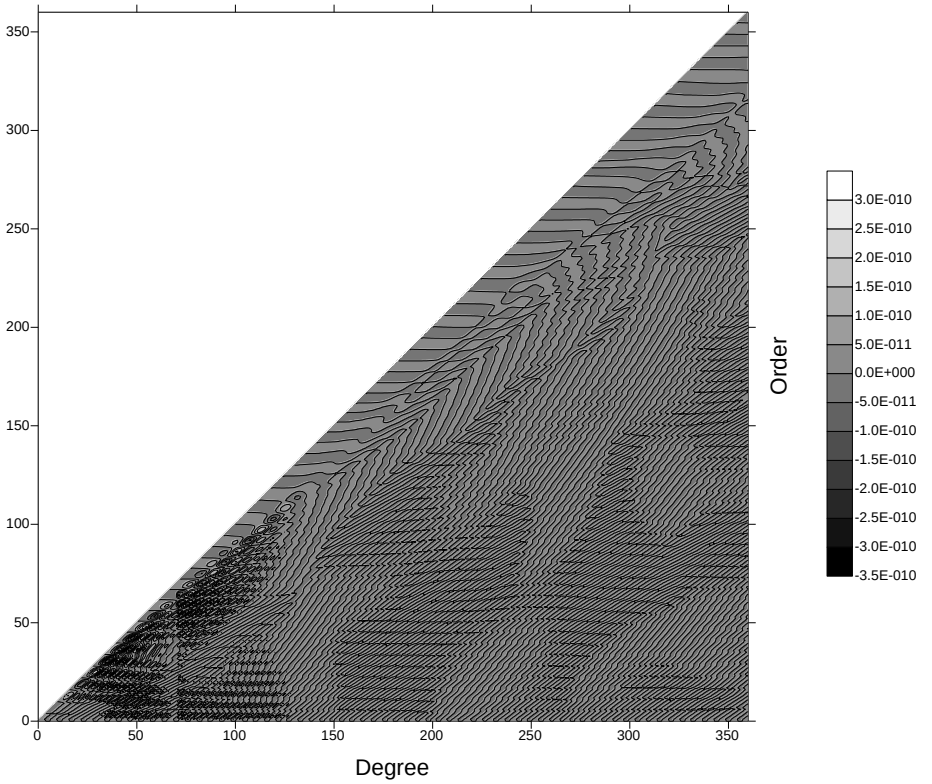

Figure (1b): Contour map for the EGM96 S-corrections

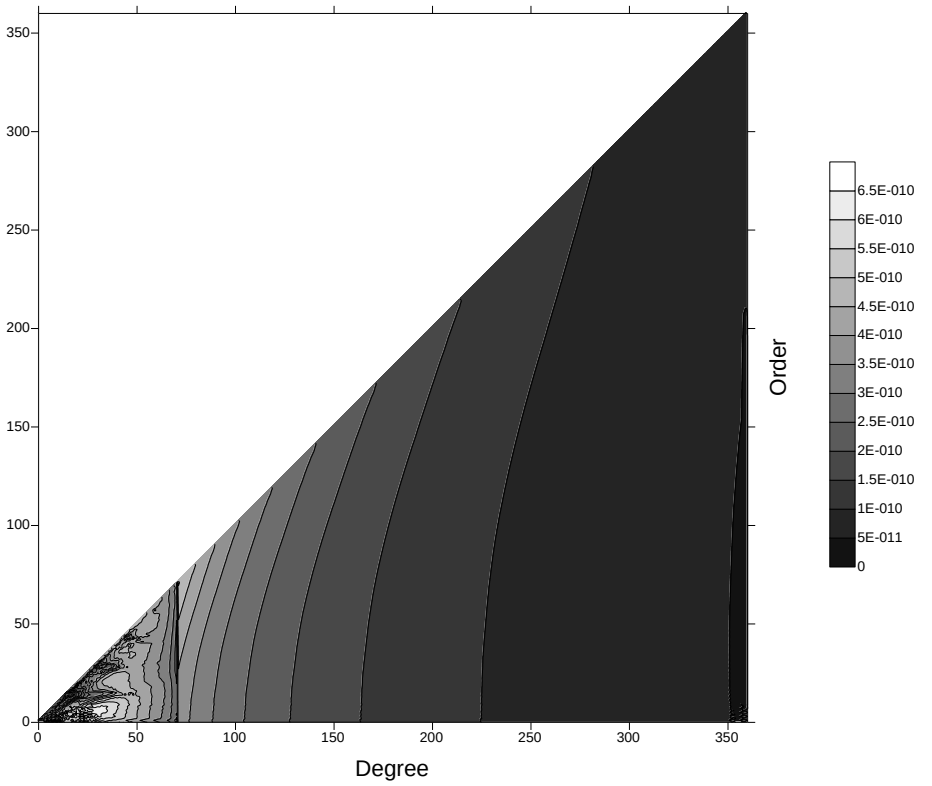

Figure (2a): Contour map for the standard errors of the EGM96 C-coefficients

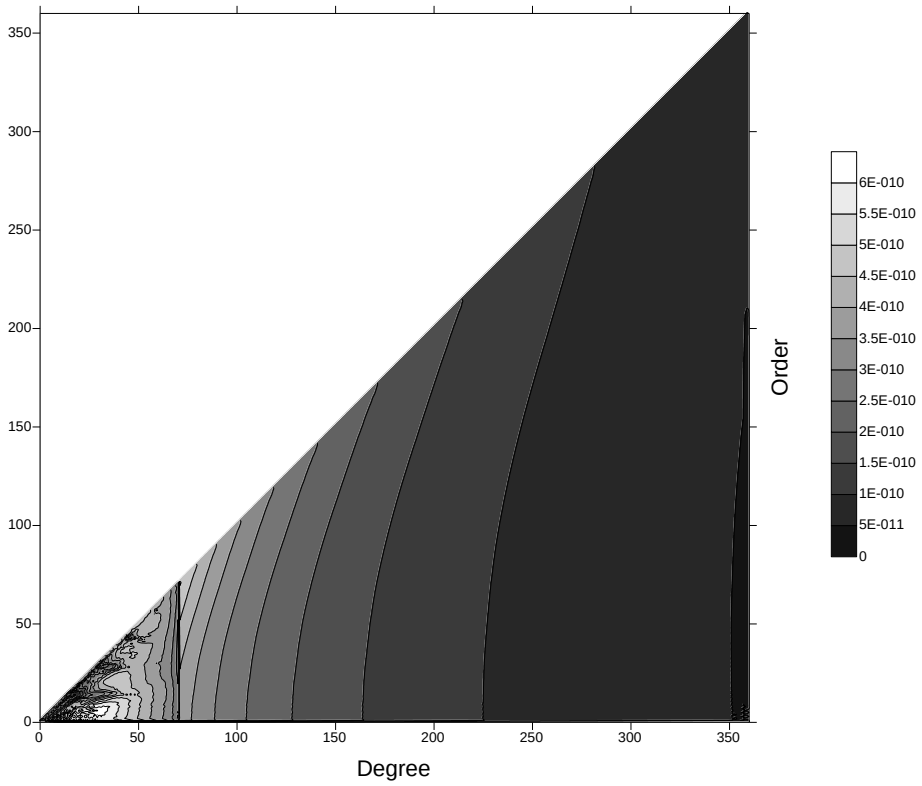

Figure (2b): Contour map for the standard errors of the EGM96 S-coefficients

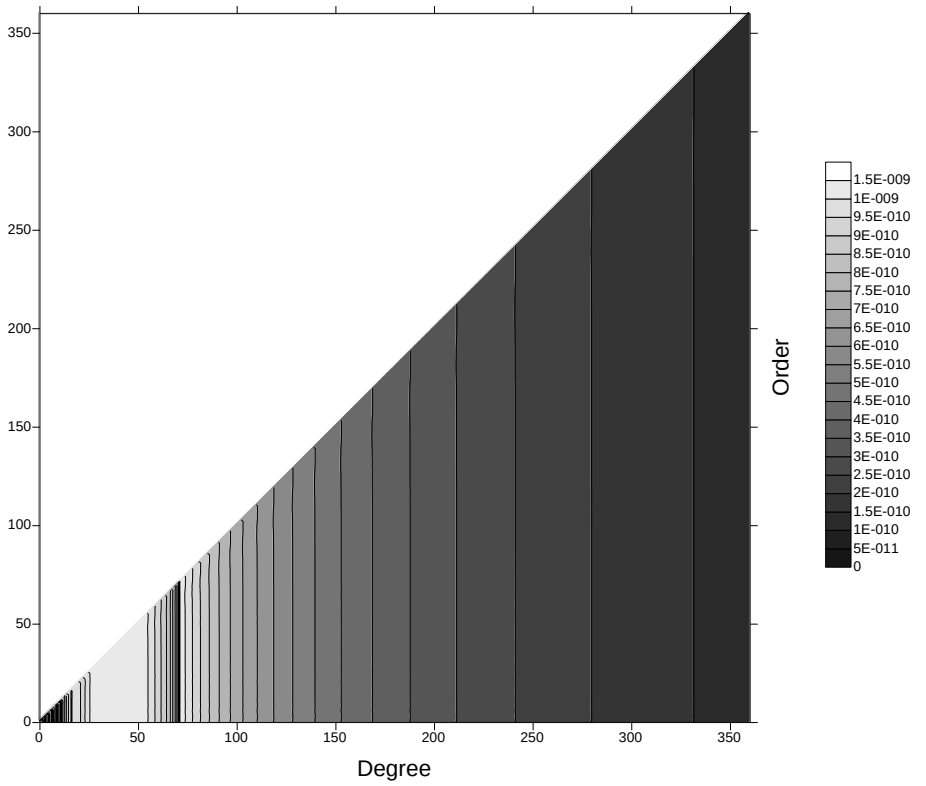

Figure (3a): Contour map for the standard errors of the EGM96EGR C-coefficients

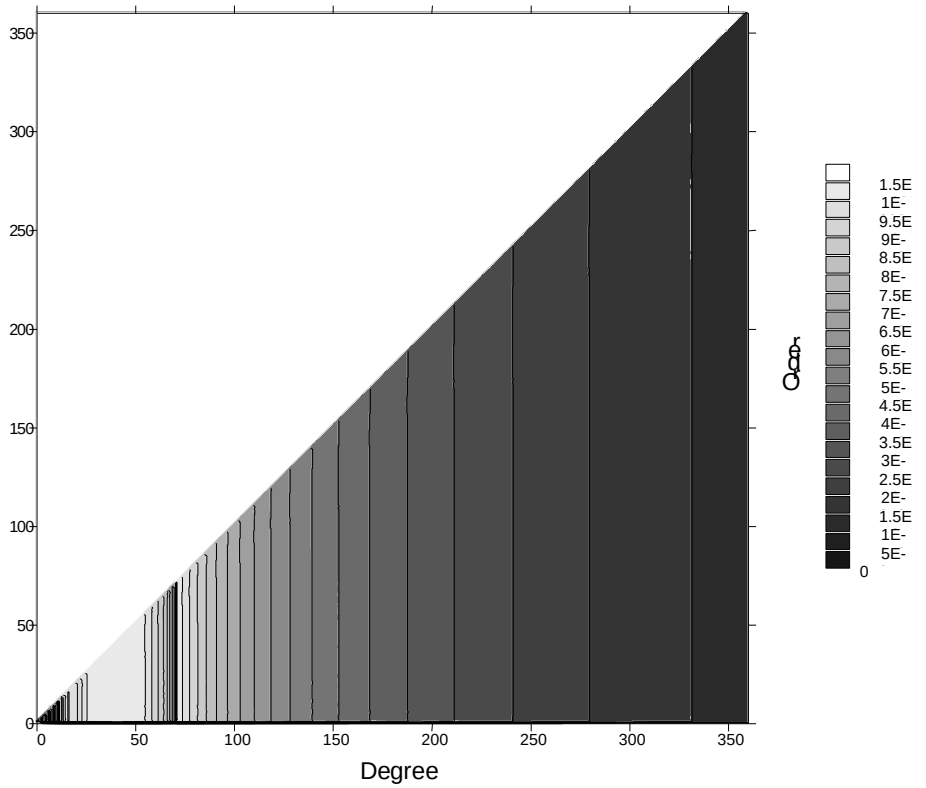

Figure (3b): Contour map for the standard errors of the EGM96EGR S-coefficients

4 The EGM96EGR and EGM96 low frequency gravity field in Egypt

In order to investigate the effect of the refinement of the EGM96 harmonic model, based on the local gravity data, the long wavelength geoidal heights N, gravity anomalies Δg, the meridian deflection components ξ and the prime vertical deflection components η were computed from both the EGM96EGR and EGM96 models in Egypt. These quantities were computed, using Eq. (2) through (5), at the nodes of a 0.5°x0.5° grid covering the Egyptian territory (the region bounded by $22°N \le \varphi \le 32°N$; $25°E \le \lambda \le 36°E$). Table (1) through (4) outline a comparison of the statistics of the four gravimetric elements, respectively, computed from both models, relative to the WGS-84 reference ellipsoid.

Table (1): EGM96EGR versus EGM96 geoidal heights in Egypt (units: meters)

Item	Mean	Std. Dev.	RMS	Minimum	Maximum
EGM96EGR N	13.862	2.902	14.162	6.870	21.010
EGM96 N	13.834	2.819	14.118	7.532	21.099
EGM96EGR N – EGM96 N	0.029	0.921	0.921	-2.098	4.893

Table (2): EGM96EGR versus EGM96 gravity anomalies in Egypt (units: mgals)

Item	Mean	Std. Dev.	RMS	Minimum	Maximum
EGM96EGR Δg	5.491	26.125	26.669	-75.360	143.063
EGM96 Δg	5.597	24.965	25.560	-125.749	152.968
EGM96EGR Δg – EGM96 Δg	-0.106	13.998	13.984	-37.385	85.289

Table (3): EGM96EGR versus EGM96 meridian deflection components in Egypt (units: arc seconds)

Item	Mean	Std. Dev.	RMS	Minimum	Maximum
EGM96EGR ξ	-0.613	4.448	4.485	-17.454	23.104
EGM96 ξ	-0.635	4.010	4.056	-16.621	22.849
EGM96EGR ξ – EGM96 ξ	0.023	2.069	2.067	-9.914	8.939

Table (4): EGM96EGR versus EGM96 prime vertical deflection components in Egypt (units: arc seconds)

Item	Mean	Std. Dev.	RMS	Minimum	Maximum
EGM96EGR η	0.574	4.073	4.109	-24.189	10.974
EGM96 η	0.557	4.216	4.248	-32.054	15.211
EGM96EGR η – EGM96 η	0.018	2.147	2.145	-8.506	10.960

From the above tables, it is clear that very significant differences exist, regarding the four considered gravimetric quantities. It seems that the refined model possesses very significant additional information, based on the incorporated new local data. Errors at the above numerical levels would be committed during the use of the EGM96 model as a reference field in a local gravity field modeling. One could expect that the long wavelength miss-modeling, using the EGM96 harmonic model, will be more obvious, if the treated gravimetric element happens to be gravity anomalies. In other words, the gravity anomaly is more sensitive to the absence of local data from a given geopotential model. This could be intuitively referred to the (n-1) magnification factor in Eq. (3). Regarding the geoidal heights and the two deflection components, this sensitivity seems to be considerably smaller. The latest statements should be taken with caution, since the situation could depend on the maximum degree of the harmonic model, the smoothness of the local gravity field and the geographical location of the region under study, implied by the relevant surface harmonic functions.

5 The far zone effect of the local modification

In order to investigate the effect of the local modification, according to the Egyptian data, on the EGM96 far zone low frequency behavior, two test remote zones far from Egypt were considered. The first test zone has previous local data contribution to the EGM96 harmonic model (Kearsley et al., 1998). It is the region of the Skagerrak Sea between Denmark and Norway and is bounded by ($56°N \le \varphi \le 59°N$; $6°E \le \lambda \le 12°E$). Conversely, the second test zone has no local data contribution to the original model (Lemoine et al., 1996). This zone lies in middle Africa and is bounded by ($5°N \le \varphi \le 15°N$; $20°E \le \lambda \le 30°E$). Again, the long wavelength geoidal heights, gravity anomalies, the meridian and the prime vertical deflection components were computed from both the EGM96EGR and EGM96 models, relative to the WGS-84 reference ellipsoid, at the nodes of two 0.5°x0.5° grids covering the two test zones.

Concerning the first test zone, Table (5) through (8) illustrate a comparison of the statistics of the four gravimetric quantities, computed from both models. Clearly, very small differences exist between the two models, regarding all the four anomalous elements, compared to those outlined in Table (1) through (4). These differences can be neglected and considered within the common measuring (and prediction) accuracy of the eventually met anomalous quantities, during a local gravity field modeling. Thus, it is clear that the addition of the local data in Egypt results in a far zone lower degree field that is almost identical to that computed from the original model, in regions that have data contribution to that model. Obviously, both harmonic models are nearly equally tuned to reflect the effect of the local data, which was previously incorporated into the original model from that zone. This can be regarded to the orthogonality among the surface harmonic functions, $Y_{nm}(\psi,\lambda)$, which is by definition used in any technique for the evaluation of harmonic coefficients. In other words, the spherical harmonic coefficients are, in a general sense, weighted mean values of the anomalous potential, which are weighted with a function that is theoretically equal to one in the considered area and zero outside this area (Tscherning, 1974). This weighting is implicitly implemented via the surface harmonics, $Y_{nm}(\psi,\lambda)$, during the expansion of the various

anomalous elements in spherical harmonic series (Eq. (1) through (5)). However, due to the inevitable uncertainties inherent into the spherical harmonic coefficients, this orthogonality can be slightly affected, and this could be the reason behind the very small differences resulting in Table (5) through (8).

Table (5): EGM96EGR versus EGM96 geoidal heights in the first far zone (units: meters)

Item	Mean	Std. Dev.	RMS	Minimum	Maximum
EGM96EGR N	39.466	2.348	39.535	34.717	44.970
EGM96 N	39.465	2.349	39.534	34.719	44.972
EGM96EGR N – EGM96 N	0.001	0.002	0.003	-0.004	0.006

Table (6): EGM96EGR versus EGM96 gravity anomalies in the first far zone (units: mgals)

Item	Mean	Std. Dev.	RMS	Minimum	Maximum
EGM96EGR Δg	6.741	16.211	17.475	-18.211	67.515
EGM96 Δg	6.729	16.216	17.474	-18.229	67.542
EGM96EGR Δg – EGM96 Δg	0.013	0.043	0.045	-0.077	0.106

Table (7): EGM96EGR versus EGM96 meridian deflection components in the first far zone (units: arc seconds)

Item	Mean	Std. Dev.	RMS	Minimum	Maximum
EGM96EGR ξ	-0.902	2.725	2.856	-8.186	4.089
EGM96 ξ	-0.904	2.726	2.858	-8.185	4.080
EGM96EGR ξ – EGM96 ξ	0.002	0.007	0.008	-0.017	-0.017

Table (8): EGM96EGR versus EGM96 prime vertical deflection components in the first far zone (units: arc seconds)

Item	Mean	Std. Dev.	RMS	Minimum	Maximum
EGM96EGR η	3.533	2.712	4.444	-5.480	10.248
EGM96 η	3.533	2.711	4.444	-5.475	10.244
EGM96EGR η – EGM96 η	0.000	0.005	0.005	-0.012	0.011

Concerning the second test zone, Table (9) through (12) show a comparison of the statistics of the four gravimetric functions, computed from both models. Again, very small differences exist between the two models, concerning the four anomalous elements, compared to those outlined in Table (1) through (4). Thus, it is clear that the addition of the local data in Egypt did not affect the second far zone computed lower degree field,

although this second zone has no data contribution to that model. It is clear that both models recover almost identically the low degree satellite terms only. Namely, both (original and refined) models recover the satellite information relevant to that zone. Among all the global satellite data, only this pertaining to the region under investigation survives (is accounted for), as a consequence of the orthogonality among the surface harmonic functions, $Y_{nm}(\psi,\lambda)$. However, the small discrepancies in this region are slightly greater than those of Table (5) through (8). This can be attributed to the fact that the orthogonality contamination by the coefficients' uncertainties is more pronounced in this second zone, since that happens to be relatively geographically nearer to Egypt than first zone.

Table (9): EGM96EGR versus EGM96 geoidal heights in the second far zone (units: meters)

Item	Mean	Std. Dev.	RMS	Minimum	Maximum
EGM96EGR N	-1.642	6.110	6.320	-12.616	10.732
EGM96 N	-1.644	6.110	6.321	-12.635	10.737
EGM96EGR N – EGM96 N	0.001	0.017	0.017	-0.036	0.046

Table (10): EGM96EGR versus EGM96 gravity anomalies in the second far zone (units: mgals)

Item	Mean	Std. Dev.	RMS	Minimum	Maximum
EGM96EGR Δg	-4.370	14.415	15.047	-52.760	46.420
EGM96 Δg	-4.378	14.434	15.068	-52.826	46.637
EGM96EGR Δg – EGM96 Δg	0.009	0.187	0.187	-0.474	0.566

Table (11): EGM96EGR versus EGM96 meridian deflection components in the second far zone (units: arc seconds)

Item	Mean	Std. Dev.	RMS	Minimum	Maximum
EGM96EGR ξ	-3.233	2.053	3.828	-9.398	4.220
EGM96 ξ	-3.231	2.056	3.828	-9.409	4.239
EGM96EGR ξ – EGM96 ξ	-0.002	0.038	0.038	-0.112	0.087

Table (12): EGM96EGR versus EGM96 prime vertical deflection components in the second far zone (units: arc seconds)

Item	Mean	Std. Dev.	RMS	Minimum	Maximum
EGM96EGR η	1.289	1.897	2.291	-4.293	7.723
EGM96 η	1.289	1.896	2.291	-4.297	7.714
EGM96EGR η – EGM96 η	0.000	0.016	0.016	-0.052	0.045

6 Spectral Analysis

In order to detect the impact of the incorporation of the local data into the harmonic model on its power spectra and error spectra, the coefficient, geoid and anomaly degree variances and error degree variances were computed for the spectral range from degree 2 to degree 360. Figure (4a) plots a comparison between the coefficient degree variances curves pertaining to the two models. According to the plot scale, the curve belonging to the refined model apparently coincides with that of the original model. In general, the two curves show the expected trend for the decrease of the coefficient power as the degree increases, according to Kaula's rule of thumb (Rapp, 1972). These similar trends ascertain that the local data corrections carry the random nature of the gravimetric anomalous signals and the spectral properties of the EGM96 model were not deformed, due to the addition of the local data. Figure (4b) gives an insight into the differences between the coefficient degree variances of both models. Clearly, the differences are relatively large in magnitude for lower degrees, randomly oscillating about zero and are damping as the degree increases. Figure (5a) gives a comparison between the two relevant geoid degree variances curves, whereas Figure (5b) plots the associated differences among the geoid degree variances. It is obvious that the curves in Figures (5a) & (5b) resemble those of Figures (4a) & (4b), respectively. This is because the geoid degree variance is simply the coefficient degree variance, scaled by R^2, as implied by Eqs. (6) and (8). Hence, the same comments concerning the coefficients degree variances for the two models are still valid for the geoid degree variances. However, the differences among power spectra in terms of geoid undulations can be considered very small.

Figure (6a) illustrates the anomaly degree variances curves pertaining to the EGM96 and EGM96EGR harmonic models. As it was the case for coefficient and geoid degree variances, the two anomaly power spectra curves almost coincide. However, an insight into the differences among the anomaly degree variances curves, Figure (6b), one could notice that the differences are firstly small for lower degrees, then they become relatively larger for intermediate degrees and finally the trend is again damping as the degree increases. This is expected, because the gravity anomalies tend to have most of its power in relatively higher degrees. As above, the differences are randomly oscillating about zero. And the differences among gravity anomaly power spectra are, in general, very small. It should be emphasized that the small differences in power spectra is only a measure of how the harmonic model has been affected, in a global sense, as a consequence of the incorporation of the local data into it. This is true, since the power spectra or even the error spectra are not functions of a specific geographical location, as it is clear from Eq. (6) to (11). Analogous to the discussions in Sections 4 & 5 concerning Egypt and the far zones, it is expected that the local near zone and far zone effects of the refinement on the power (and error) spectra would only be obvious in a local covariance function modeling.

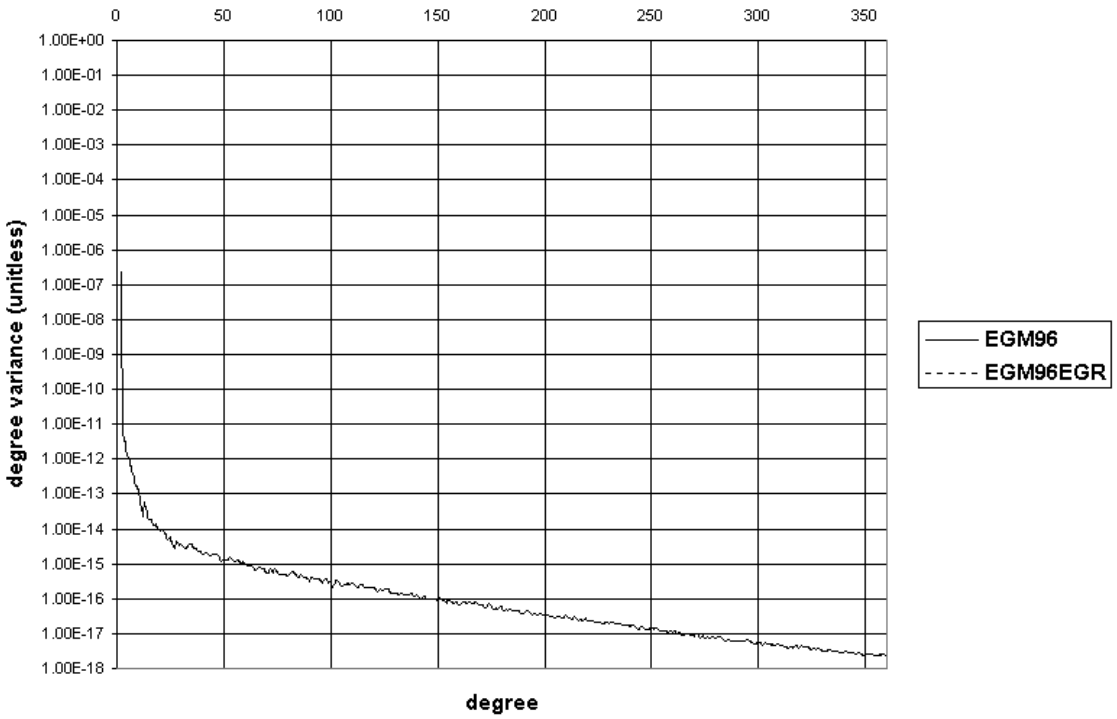

Figure (4a): The coefficient degree variances curves for the EGM96EGR and EGM96 harmonic models (log scale)

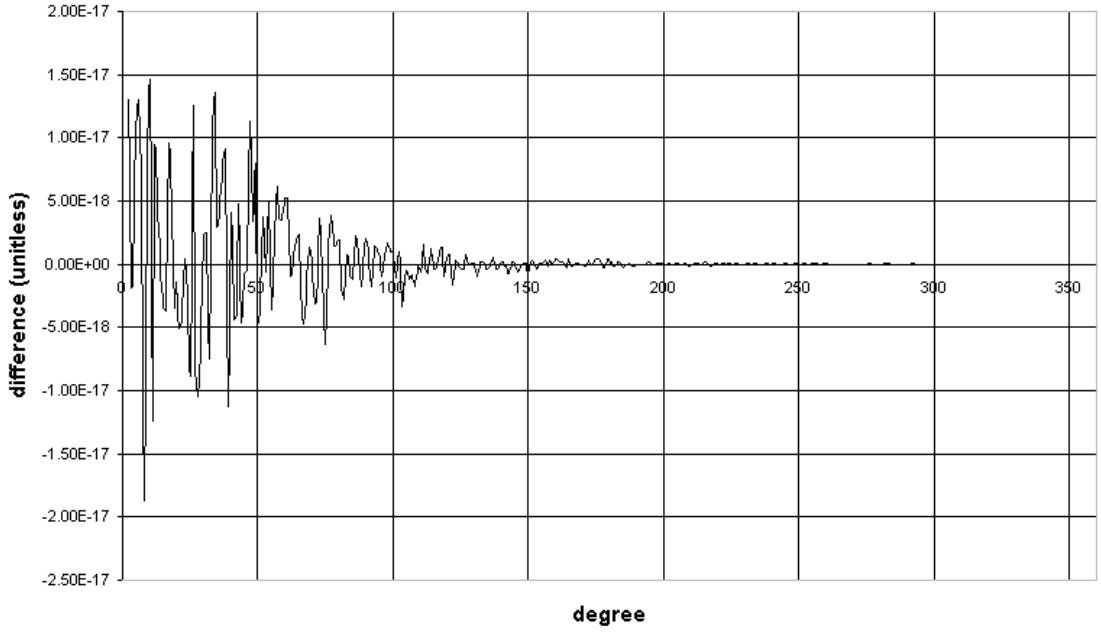

Figure (4b): The differences among the coefficient degree variances for the EGM96EGR and EGM96 harmonic models

Figure (4)

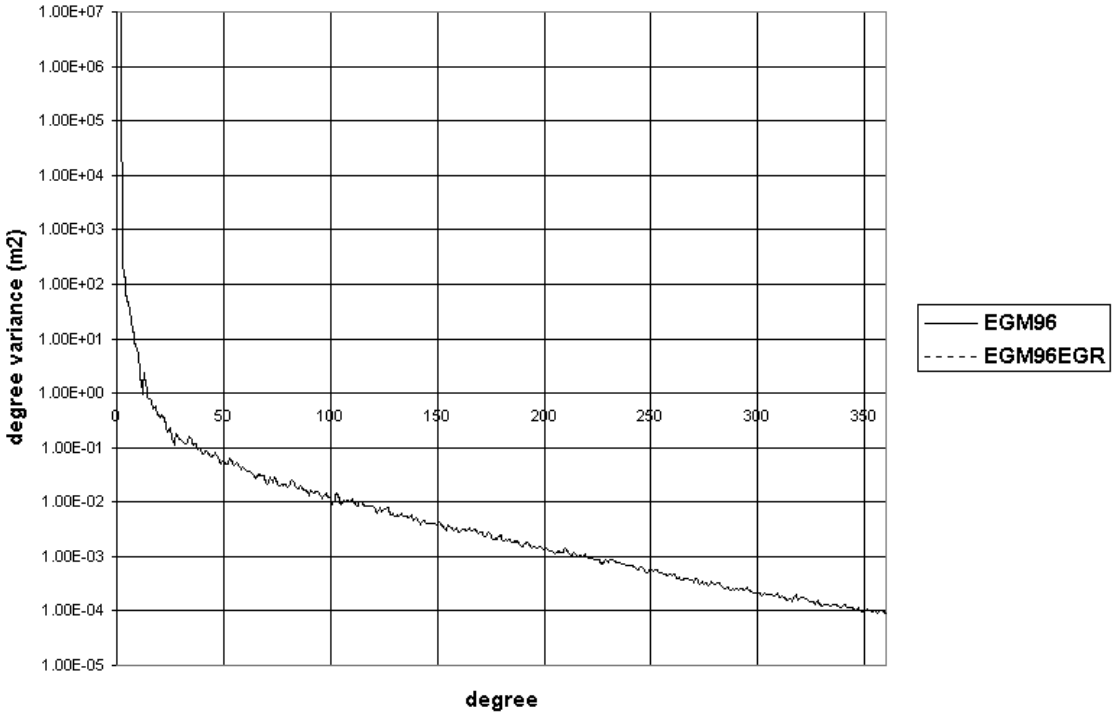

Figure (5a): The geoid degree variances curves for the EGM96EGR and EGM96 harmonic models (log scale)

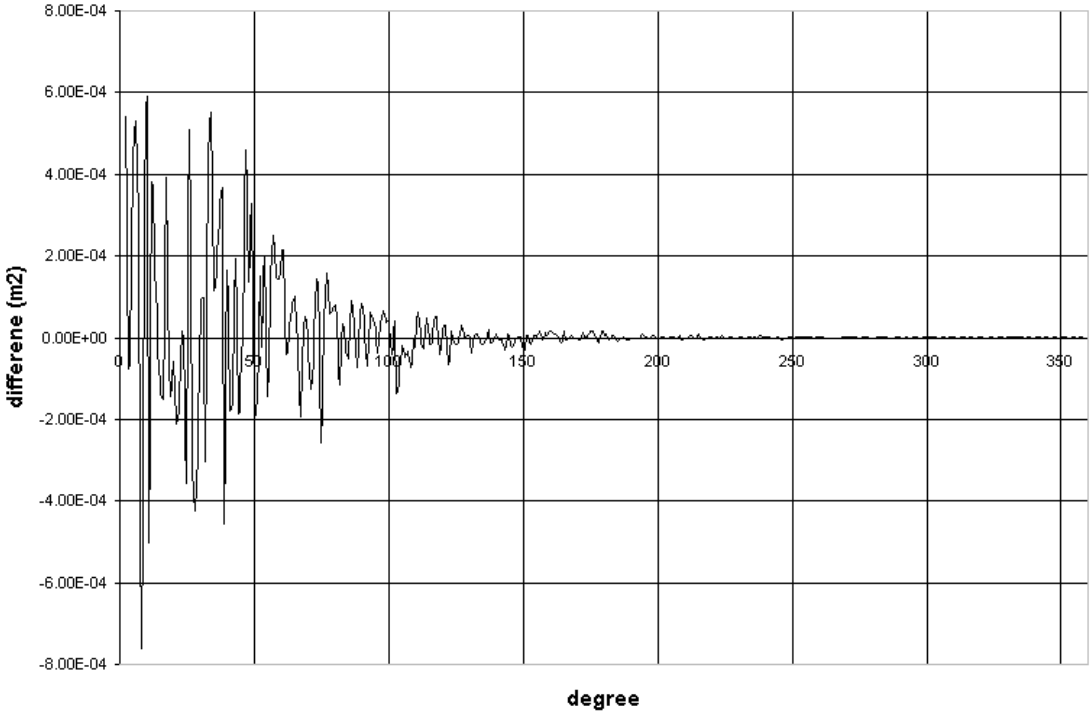

Figure (5b): The differences among the geoid degree variances for the EGM96EGR and EGM96 harmonic models

Figure (5)

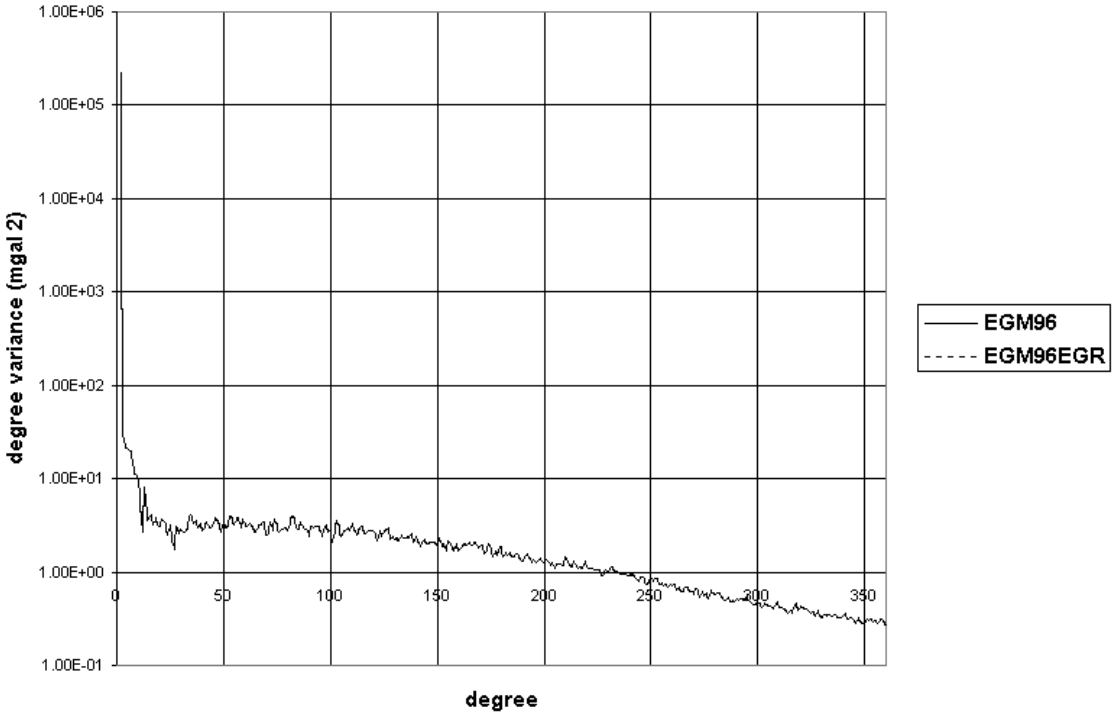

Figure (6a): The gravity anomaly degree variances curves for the EGM96EGR and EGM96 harmonic models (log scale)

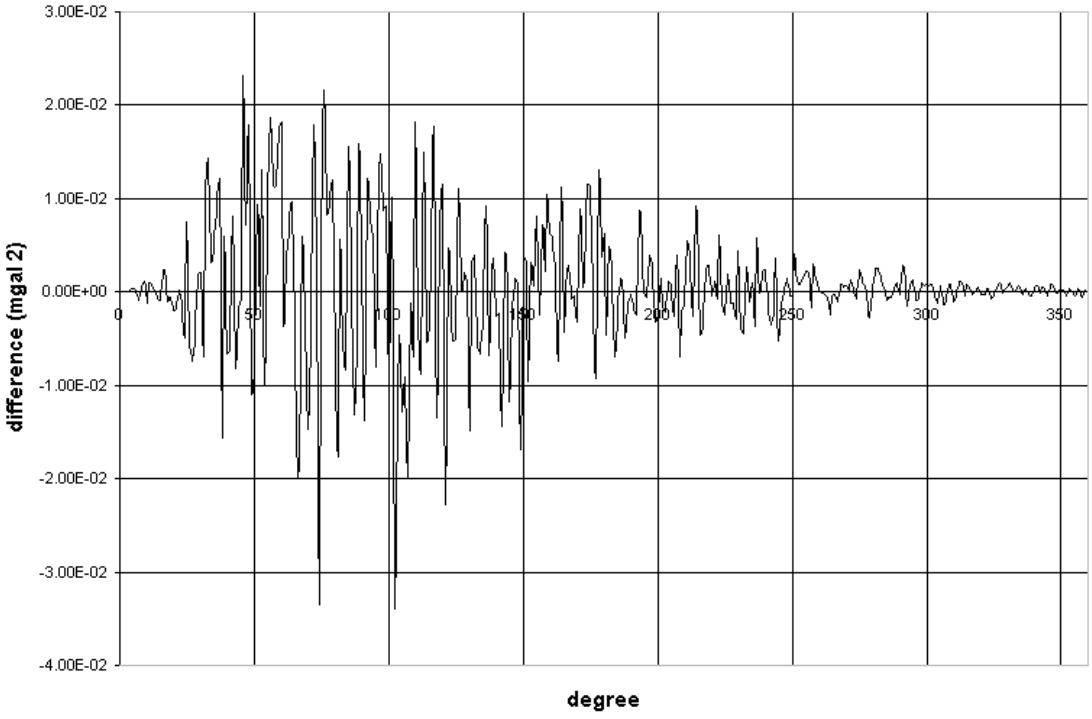

Figure (6b): The differences among the gravity anomaly degree variances for the EGM96EGR and EGM96 harmonic models (log scale)

Figure (6)

Finally, Figures (7), (8) and (9) show comparisons regarding the two models' coefficient, geoid and anomaly error degree variances curves, respectively. It is clear how the error degree variances , and hence, the error estimation characteristics of the refined model have the same structure as those of the original one. This was previously noticed in Figures (2a &2b) and (3a &3b). Also Figure (7) through (9) ensure that there exist two error spectral bands with different characteristics. However, due to the previously discussed pessimistic nature of the refined model error estimates, the coefficient, geoid and anomaly error spectra of the refined model are considerably larger than those of the original model.

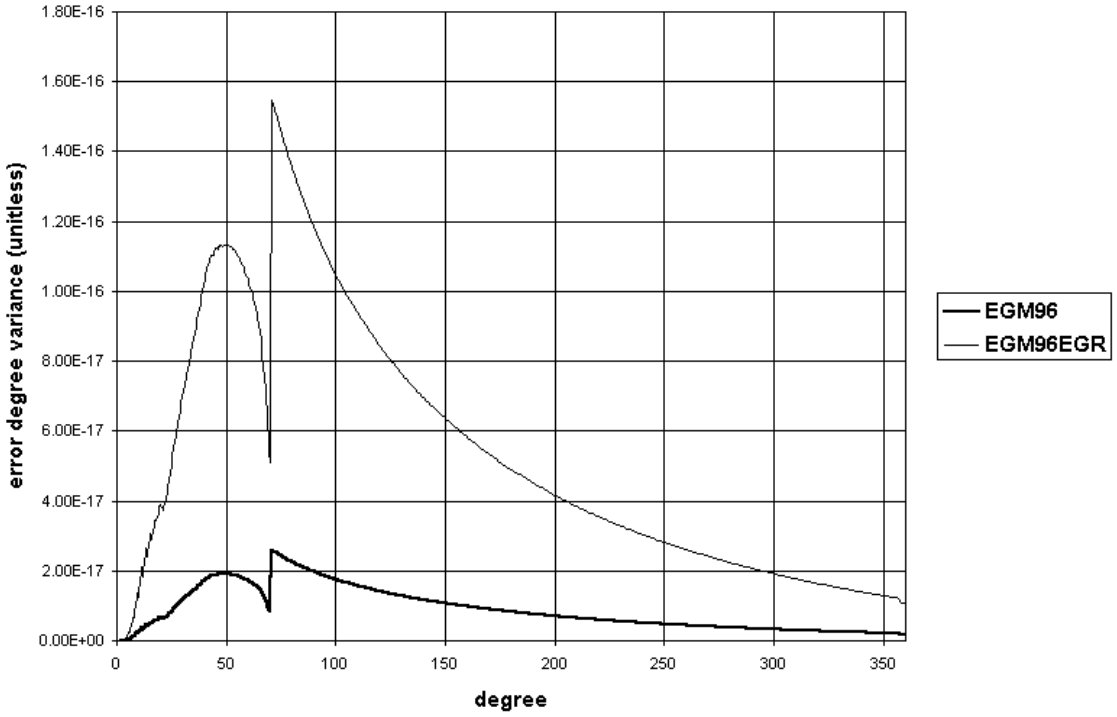

Figure (7): The coefficient error degree variances curves for the EGM96EGR and EGM96 harmonic models

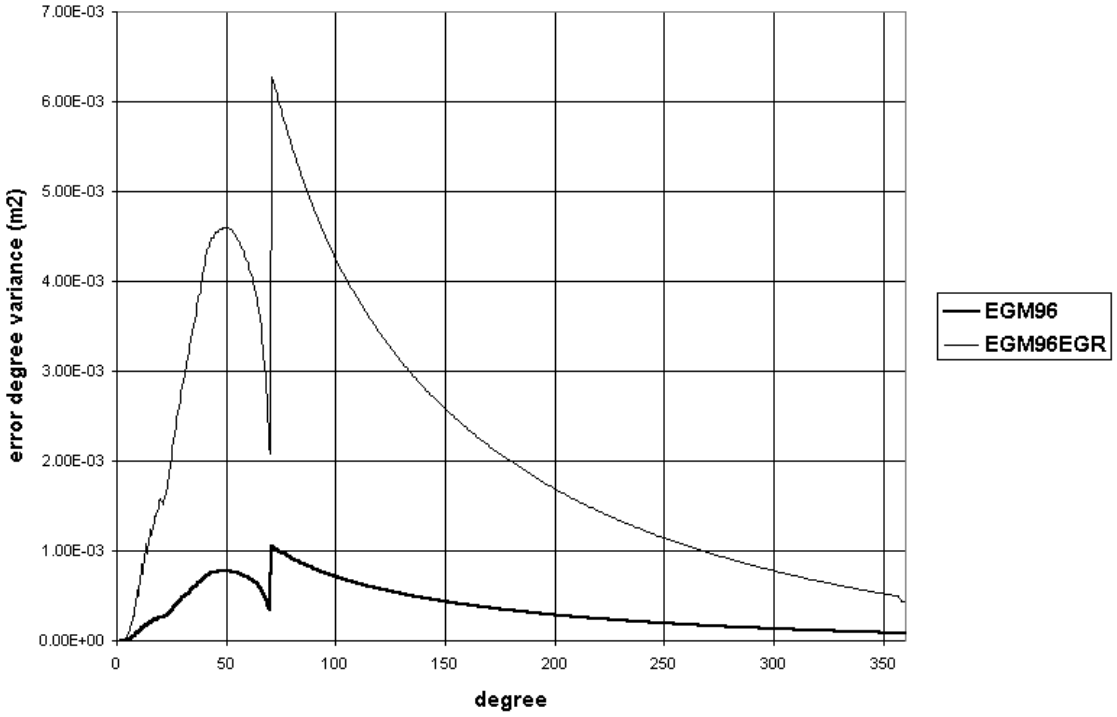

Figure (8): The geoid error degree variances curves for the EGM96EGR and EGM96 harmonic models

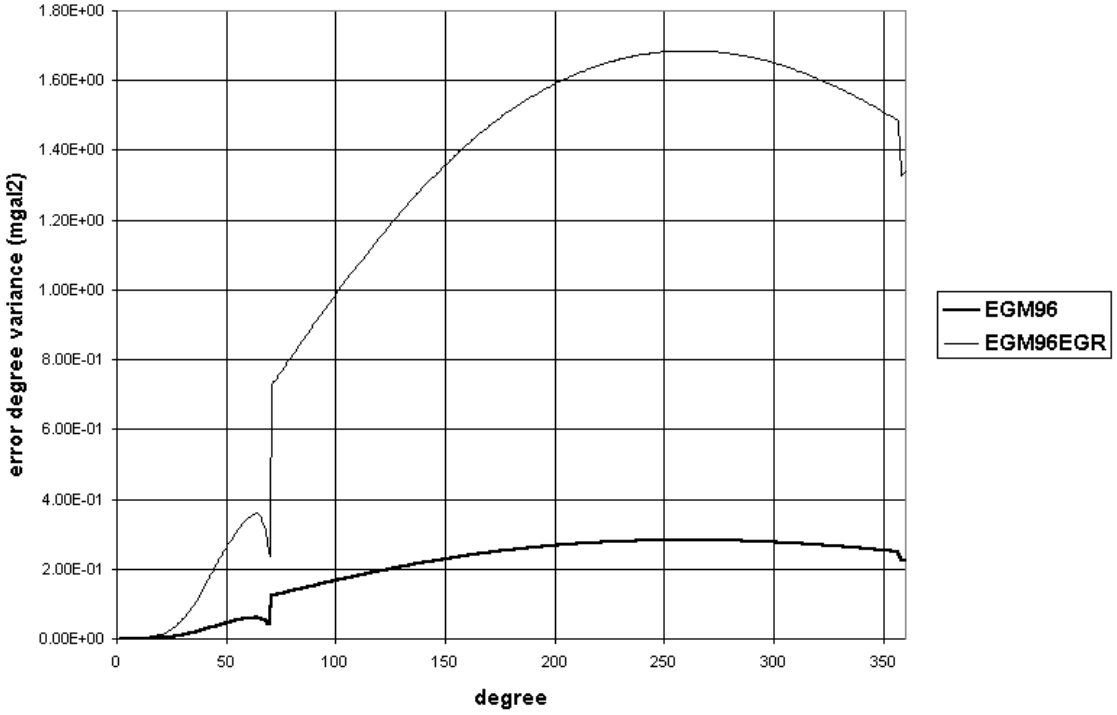

Figure (9): The gravity anomaly error degree variances curves for the EGM96EGR and EGM96 harmonic models

7 Conclusions

Based on the current study, it is obvious that concerning Egypt, the EGM96EGR harmonic model have very significant local low frequency information over the EGM96. This was found regarding the four investigated gravimetric quantities. It is also concluded that the addition of new local data, to a specific existing harmonic model, has practically no effect on the computed far zone low frequency information. This was proved to be true for far zones with or without previous data contribution to the EGM96 model. Based on the spectral analysis performed on the two models, the refined model power spectra trends almost coincide with those of the original model. The differences among the coefficient, geoid and anomaly power spectra of the two models were found to be in general randomly oscillating about zero and damping as the degree increases. Specifically, the differences regarding the geoid and gravity anomaly power spectra were found to be small. However, due to the pessimistic nature of LSC coefficients' error estimates, the error degree variances (error spectra) of the refined model were greater than those of the original one. It is recommended to use the EGM96EGR model in local gravity field modeling in the near future. By implementing this task, the local effect of the power and error spectra would be clear during the covariance function modeling.

References

Amin, M.M. (2002): "Evaluation of Some Recent High Degree Geopotential Harmonic Models in Egypt", Port-Said Engineering Research Journal PSERJ, Published by Faculty of Engineering, Suez Canal University, Port-Said, Egypt.

Amin, M.M.; El-Fatairy, S.M. and Hassouna, R.M. (2002): "A Better Match Of The EGM96 Harmonic Model For The Egyptian Territory Using Collocation", Port-Said Engineering Research Journal PSERJ, Published by Faculty of Engineering, Suez Canal University, Port-Said, Egypt.

Heiskanen, W.A. and Moritz, H. (1967): "Physical Geodesy", W.H. Freeman and Company, San Francisco and London.

Kearsley, A.H.W.; Forsberg, R.; Olesen, A.; Bastos, L; Hehl, K.; Meyer, U. and Gidskehaug, A. (1998): "Airborne gravimetry used in precise geoid computations by ring integration", Journal of Geodesy, Vol. 72: 600-605.

Lemoine, F.G.; Smith, D.E.; Kunz, L.; Smith, R.; Pavlis, E.C.; Pavlis, N.K.; Klosko, S.M.; Chinn, D.S.; Torrence, M.H.; Williamson, R.G.; Cox, C.M.; Rachlin, K.E.; Wang, Y.M.; Kenyon; S.C.; Salman, R.; Trimmer, R.; Rapp, R.H. and Nerem, R.S. (1996): "The Development of the NASA GSFC and NIMA Joint Geopotential Model", Proceedings paper for the International Symposium on Gravity, Geoid and Marine Geodesy (GRAGEOMAR 1996), The University of Tokyo, Tokyo, Japan, September 30-October 5.

Rapp, R.H. (1972): "Geopotential Coefficient Behavior to High Degree and Geoid Information by Wavelength", Report No. 180, Department of Geodetic Science, The Ohio State University.

Tscherning, C.C. (1974): " A FORTRAN IV program for the determination of the anomalous potential using stepwise least squares collocation", Report No. 212, Department of Geodetic Science, The Ohio State University.

Tscherning, C.C. (1993): "An experiment to determine gravity from geoid heights in Turkey", GEOMED Report No. 3.

Tscherning, C.C. (2001): "Computation of spherical harmonic coefficients and their error estimates using least-squares collocation", Journal of Geodesy, Vol. 75, No. 1: 12-18.